

High Pressure Raman, Optical Absorption, and Resistivity Study of SrCrO_4

Malik A. Hakeem,[†] Daniel E. Jackson,[‡] James J. Hamlin,[‡] Daniel Errandonea,[§] John E. Proctor,^{*,†,||} and Marco Bettinelli^{||}

[†]School of Computing, Science and Engineering, University of Salford, Manchester M5 4WT, United Kingdom

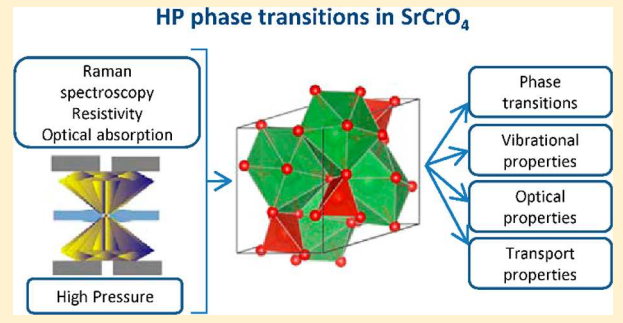
[‡]Department of Physics, University of Florida, Gainesville, Florida 32611, United States

[§]Departamento de Física Aplicada-ICMUV, MALTA Consolider Team, Universidad de Valencia, Edificio de Investigación, C/Dr. Moliner 50, Burjassot 46100, Valencia, Spain

^{||}Photon Science Institute and School of Electrical & Electronic Engineering, University of Manchester, Oxford Road, Manchester M13 9PL, United Kingdom

[†]Luminescent Materials Lab, Department of Biotechnology, University Verona and INSTM, UdR Verona, Strada Le Grazie 15, 37134 Verona, Italy

ABSTRACT: We studied the electronic and vibrational properties of monazite-type SrCrO_4 under compression. The study extended the pressure range of previous studies from 26 to 58 GPa. The existence of two previously reported phase transitions was confirmed at 9 and 14 GPa, and two new phase transitions were found at 35 and 48 GPa. These transitions involve several changes in the vibrational and transport properties with the new high-pressure phases having a conductivity lower than that of the previously known phases. No evidence of chemical decomposition or metallization of SrCrO_4 was detected. A tentative explanation for the reported observations is discussed.



1. INTRODUCTION

Photocatalytic materials which respond to ultraviolet and visible light have gained much attention during recent years. Among them, chromates of general formula ACrO_4 , where A is a divalent metal (e.g., Sr, Ba, and Pb), were found to have excellent optical-absorption properties, a high photocatalytic activity, and a band gap energy near 2.5 eV. Such unique properties make ACrO_4 chromates useful not only in photocatalysis but also in a wide range of applications, including photosensitization, photoluminescence, and scintillation.^{1–4} Strontium chromate (SrCrO_4) has the advantage against its Ba and Pb analogues of not being toxic to humans.

The crystal structure of SrCrO_4 at ambient conditions is well-known, being isomorphic to the monazite structure (space group $P2_1/n$).⁵ It consists of Sr atoms coordinated by nine oxygen atoms and distorted CrO_4 tetrahedral units. Its main physical properties at atmospheric conditions have been studied experimentally and theoretically.^{6–8} SrCrO_4 was characterized as a semiconductor material with a band gap energy of 2.45 eV.⁷ The frequencies of the Raman-active phonon modes were accurately determined.⁷ Such information has contributed considerably to establishing the composition of late 19th to early 20th century oil paintings.⁹

The effect of compression in the properties of SrCrO_4 was recently studied up to 26 GPa.¹⁰ In these studies, evidence of two phase transitions at 8–9 and 10–13 GPa was found. The

crystal structures of the high-pressure (HP) phases were assigned to the tetragonal scheelite-type and monoclinic AgMnO_4 -type structures. The influence of these transitions in the lattice vibrations and electronic band-structure was also established.¹⁰ The interest in studies comes from the fact that they were shown to be an effective instrument for deepening the understanding of properties of oxides related to SrCrO_4 .^{11–15} The extension of studies in SrCrO_4 toward higher pressures is of interest for several reasons: to search for new phase transitions, including possible pressure-induced amorphization¹⁶ and metallization,¹⁷ and the determination of possible effects of pressure on the chemical composition.¹⁸ All these phenomena were found to occur in oxides related to SrCrO_4 at pressures not far from 20 GPa.

Here, we present a HP Raman study of monazite-type SrCrO_4 up to 58 GPa. The study is combined with optical-absorption measurements up to 32 GPa and resistivity measurements up to 50 GPa. In the next sections, we describe the experimental techniques and report and discuss the results of the present experiments. Evidence of two previously unknown phase transitions is reported. The behavior of SrCrO_4 under HP is compared with that of related oxides.

Received: February 8, 2018

Published: June 21, 2018

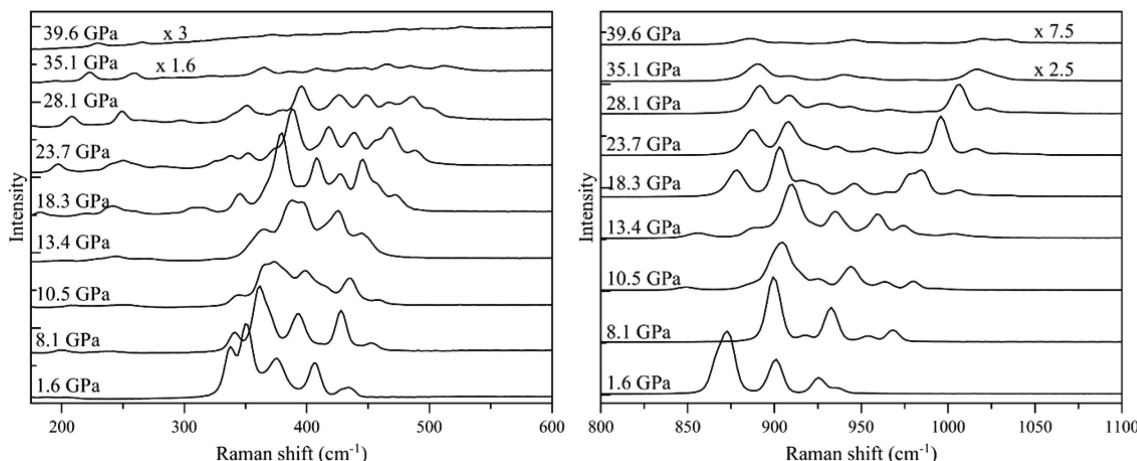


Figure 1. Raman spectra measured in SrCrO_4 at selected pressures. The left and right panels correspond to the two frequency regions described in the text. The magnification of spectra measured at 35.1 and 39.6 GPa is indicated in the figures.

2. EXPERIMENTAL METHODS

Single crystals of SrCrO_4 were grown by solid-state reaction following the procedure described in ref 10. The high purity of the synthesized crystals was confirmed by energy-dispersive X-ray spectroscopy measurements carried out using a transmission electron microscope operated at 200 keV. The crystal structure was verified by powder X-ray diffraction using $\text{Cu K}\alpha$ radiation. It was assigned to the well-known monazite-type structure, with unit-cell parameters: $a = 7.065(7)$ Å, $b = 7.376(7)$ Å, $c = 6.741(7)$ Å, and $\beta = 103.1(1)^\circ$, in good agreement with the literature.^{5,7}

For the HP Raman measurements, we used a diamond-anvil cell (DAC) equipped with 250 μm diameter diamond gaskets. Rhenium gaskets were indented to a thickness of 40 μm . The pressure chamber was a 100 μm diameter hole drilled in its center. Ruby chips were loaded together with the sample for pressure determination using the calibration reported by Dewaele et al.¹⁹ N_2 was employed as a pressure-transmitting medium (PTM).²⁰ Special caution was taken during the DAC loading to avoid sample bridging between the anvils.^{21,22} Three independent Raman experiments were carried out. Raman spectra were measured under compression to 58 GPa. At each pressure, Raman spectra were collected using a single grating HORIBA Jobin Yvon iHR320 spectrometer with a 1200 gr/mm and a nitrogen-cooled HORIBA Jobin Yvon Symphony CCD. The backscattering geometry was used with a 532 nm laser (spot size of the order of 1 μm). A 20 \times magnification objective was employed to focus the laser on sample and collect the Raman signal. The incident power on the sample (10 mW) was kept constant in the sample along the Raman measurements. The spectral resolution was better than 6.5 cm^{-1} full width at half-maximum.²³ Raman spectra were analyzed using MagicPlot Student 2.5.1 software. The background was subtracted, and Lorentzian curves were fitted to peaks emanating from SrCrO_4 .

For optical-absorption measurements, the same DAC setup was employed except that argon²⁴ was used as PTM instead of N_2 . The measurements were carried out using a confocal setup built using an Ocean Optics DH-2000 light-source, Cassegrain objectives, and a USB2000 UV-vis-NIR spectrometer from Ocean Optics.^{25,26} The absorption spectra were computed at selected pressures from the transmittance spectra, which were collected using the sample-in sample-out method.^{27,28} The pressure was determined using the ruby scale; the maximum pressure achieved was 32 GPa.

Resistivity measurements were carried out up to 50 GPa using a Almax-Easylab OmniDac gas-membrane-driven DAC. The pressure was calibrated using the fluorescence of ruby. Resistivity was measured using a designer anvil²⁹ with a culet diameter of approximately 180 μm . A powdered sample was loaded directly into a stainless steel gasket with no insulating material separating the sample from the gasket. Resistance was measured with a Lakeshore

Model 370 AC resistance bridge using a two-probe setup. From measurements across different combinations of the wires and previous experiments with the same anvils, it was estimated that the contact resistances never exceeded 10% of the total resistance. The sample resistivity, ρ , is obtained using the equation $\rho = (\pi t R / \ln 2)$, where R is the resistance and t is the estimated thickness of the sample. We used the same procedure and experimental setup previously to obtain accurate results on the pressure dependence of the resistivity in PbCrO_4 and other semiconducting materials.^{30,31}

3. RESULTS AND DISCUSSION

a. Raman Spectroscopy. The Raman spectrum of SrCrO_4 under compression was studied in the past by our group up to 26 GPa.¹⁰ To avoid redundancies, we concentrate here on new results from 26 to 58 GPa. The Raman-active modes of SrCrO_4 are located in three isolated frequency regions in which modes have very different intensities. The strongest modes, which are associated with internal stretching vibrations of the CrO_4 tetrahedron, are located above 800 cm^{-1} (high-frequency region).^{7,10} Then, there are modes from 290 to 550 cm^{-1} (intermediate frequency region), which originate from internal bending vibrations of the CrO_4 ion, and whose intensity is approximately five times weaker than that of the high-frequency modes. Finally, there is a group of weak modes below 290 cm^{-1} (low-frequency region), which involves movements of the Sr atoms and CrO_4 ions as rigid units. The clearest evidence of phase transitions and chemical decomposition in SrCrO_4 and other monazite-type chromates is expected to be detected in the 290–550 and 800–1100 cm^{-1} regions.^{10,32} In particular, the high-frequency phonons are very sensitive to coordination changes for the Cr atom. Both the number of modes and the frequencies of the modes could change as a consequence of a structural transition. Based upon this fact, we focused the study in two sections of the spectrum of SrCrO_4 , the medium wavenumber region from 290 to 550 cm^{-1} (which we extended from 200 to 600 cm^{-1}) and the high wavenumber region from 800 to 1100 cm^{-1} , using longer acquisition times in the first region.

In Figure 1, we show a selection of Raman spectra measured under compression. Evidence of the first transition can be seen at 10.5 GPa. See, for instance, the changes in the left panel when comparing the spectra at 8.1 and 10.5 GPa and the new peak appearing near 850 cm^{-1} (right panel). This Raman spectrum corresponds to the coexistence of the monazite and

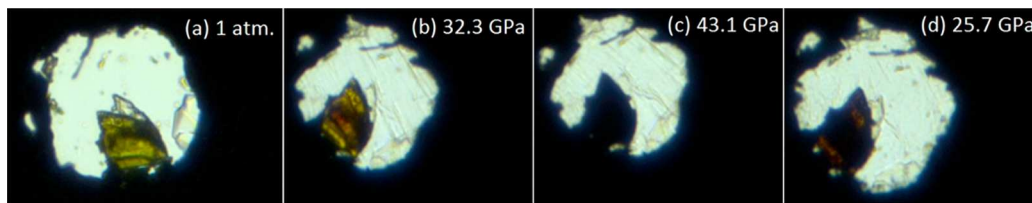


Figure 2. Images of SrCrO_4 crystal under compression. (a) SrCrO_4 at ambient pressure visible in yellow-orange color. (b) SrCrO_4 at 32.3 GPa experiencing a color change from yellow to orange at the center. (c) Color change to black at 43.1 GPa. (d) SrCrO_4 at 25.7 GPa on decompression, experiencing a color change from black to orange but having permanent cracks.

scheelite phases of SrCrO_4 .¹⁰ The second transition (to AgMnO_4 -type SrCrO_4) is illustrated by the spectrum measured at 18.3 GPa. Notice for instance the new peaks at low frequencies (left panel) and the differences between the spectra measured at 13.4 and 18.1 GPa in the right panel. These results confirm previously published results.¹⁰ The first transition corresponds to the monazite–scheelite transition previously reported at 9 GPa,¹⁰ the second transition to the scheelite– AgMnO_4 -type transition reported at 13 GPa¹⁰ but taking place at slightly higher pressure (beyond 13.4 GPa) in this work. From this pressure up to 35.1 GPa, we observed only a gradual evolution with pressure of the Raman spectrum. At this pressure, we detected qualitative changes in the Raman spectrum. The changes are reversible and include the increase of the number of Raman modes detected and the decrease of the intensity of the Raman signal. The mentioned changes can be clearly seen by comparing the spectra at 28.1 and 35.1 GPa in Figure 1. A possible explanation for this observation is the existence of a third phase transition (to a phase we name as phase IV). Such hypothesis is supported by the results of our optical and resistivity experiments, discussed in the next section. Because at 35.1 GPa the experimental conditions were not quasi-hydrostatic,²⁰ there is a possibility that the phase transition at 35.1 GPa could be triggered by the presence of large strains.³³ The study in detail of such hypothesis is beyond the scope of the present work.

Upon further compression, we did not observe any qualitative change in the Raman spectrum up to 48 GPa. However, the Raman signal intensity gradually decreases as pressure is increased until there is no detectable Raman signal past 48 GPa, and the sample appeared black. We consider this observation as the evidence of the existence of a possible fourth phase transition to a phase we name as phase V. The blackening of the sample starts at 43 GPa, is gradual, and can be caused by precursor defects of the fourth phase transition.³⁴ This phenomenon is reversible, albeit with significant hysteresis (the Raman spectrum is not recovered until 26 GPa upon decompression). However, permanent cracks are induced in the crystal, which remain on pressure release. This is typical of a first-order phase transition,³⁵ but is also observed following pressure-induced amorphization (defined as the loss of long-range order).³⁶ In Figure 2, we show pictures of the sample to illustrate it.

We now discuss the possible decomposition of SrCrO_4 under compression. Pressure-induced decomposition is expected to occur when the decomposition products occupy less volume than any polymorph of the parent material.³⁷ Usually this phenomenon is irreversible and leads to the appearance of Raman modes that cannot be assigned to the parent material.³⁸ In our case, no irreversible changes were detected. The Raman spectrum of SrCrO_4 is recovered upon decompression with no

additional modes present, ruling out the possible decomposition of SrCrO_4 . Another phenomenon that should be considered is pressure induced amorphization, which usually occurs by the kinetic hindrance of a phase transition.³⁷ However, our experimental findings indicate that SrCrO_4 does not undergo pressure induced amorphization. In oxides related to monazite, pressure-induced amorphization usually induces a precipitous decline in Raman intensity and the appearance of diffuse bands which remain upon pressure release instead of the original Raman peaks.³⁹ In our case, the Raman signal decreases below the detection limit at 48 GPa; however, the phenomenon is fully reversible, so it cannot be assigned to amorphization. Notice that the recrystallization of an amorphous solid at room temperature is very unusual, being reported up to now only in molecular compounds such as SiH_4 .⁴⁰ This phenomenon is related to the bond directionality of these compounds, which differs from that of SrCrO_4 . Additionally, the typical amorphous Raman signal has not been detected in our measurements. We believe that the loss of the Raman signal is related to the occurrence of the fourth phase transition. In the phase found beyond 48 GPa, the formation of a large population of cracks in the crystal, described above, triggers a disorder-induced decrease in intensity of the Raman scattering.⁴¹ Such an explanation should be confirmed by future studies. Of particular relevance would be the performance of HP-XRD studies using He as pressure-medium, HP-HT XRD measurements, and X-ray absorption studies at Sr k-edge to explore possible coordination changes associated with the fourth phase transition.

We now discuss the mode assignment of Raman modes in the AgMnO_4 -type phase and the pressure dependence of the modes. We focus only on bending and stretching modes of the CrO_4 tetrahedron (i.e., those with frequencies $>300 \text{ cm}^{-1}$). According to the crystal symmetry, this phase has thirty-six Raman-active phonons ($\Gamma = 18 \text{ A}_g + 18 \text{ B}_g$).¹⁰ Following density functional theory calculations,¹⁰ eight of these modes correspond to internal stretching modes of the CrO_4 tetrahedron and ten to bending vibrations of the same octahedron.¹⁰ The stretching (bending) vibrations are in the high-frequency (intermediate-frequency) region of the Raman spectrum. However, in previous measurements,¹⁰ ten modes (instead of eight) were reported in the high-frequency region and eight modes (instead of ten) in the intermediate frequency region. Here, we found the expected number of modes in each of the frequency regions of the Raman spectrum. The results from present and previous¹⁰ experiments are compared in Table 1. The agreement in frequencies is quite good. The two modes not detected in the previous study¹⁰ are the A_g modes with frequencies 340 and 375 cm^{-1} at 11.7 GPa, which are two weak modes. The two extra modes detected previously in the high-frequency region are the two weakest modes which

Table 1. Wave Numbers (ω_0) Determined at 11.7 GPa for Raman Modes of AgMnO_4 -type SrCrO_4 (in cm^{-1}) Including Mode Assignment^a

mode	ω_0 previous work	ω_0 this work	ω_1 this work	ω_2 this work
A_g		340	1.30	0.01
B_g	354	353	2.04	-0.03
B_g	371	371	1.10	0.02
A_g		375	1.48	0.01
B_g	387	387	1.67	-0.01
A_g	395	396	2.38	-0.02
B_g	411	411	1.93	0.02
A_g	419	419	1.52	0.02
B_g	434	434	1.88	0.02
A_g	445	446	2.67	-0.01
A_g	852	851	2.92	-0.02
B_g	890	890	2.58	-0.02
A_g	904	904	2.65	-0.02
A_g	918	918	4.02	-0.07
overtones	927	927	2.60	-0.03
B_g	933	933	3.87	-0.05
B_g	954	954	3.41	-0.03
A_g	969	969	3.44	-0.03
B_g	996	997	2.99	-0.03
overtones	1002	1002	4.20	-0.08

^aThe pressure dependence of the frequency of each mode is described by $\omega(P) = \omega_0 + \omega_1 \Delta P + \omega_2 \Delta P^2$, with $\Delta P = P - 11.7$ GPa. The wave numbers determined previously¹⁰ are included for comparison. The overtones (see text) are also included.

probably correspond to Raman overtones.¹⁰ Their frequencies are 927 and 1002 cm^{-1} at 11.7 GPa, and not those previously proposed (851 and 891 cm^{-1}). The frequencies we propose here for the overtones, within the accuracy of measurements, agree with the sums of the frequencies of two lower frequency A_g modes:¹⁰ (852 + 78) cm^{-1} and (918 + 82) cm^{-1} , respectively. The pressure coefficients obtained for the overtones differ by 30% from the sum of the respective pressure coefficients of the Raman modes involved in the overtones. The reason for this is possibly the very low intensities of the overtones and consequent inaccuracy in the determination of their pressure dependence.

Regarding the pressure dependence of the Raman frequencies, the obtained results are shown in Figure 3. There, it can be seen that most of the modes follow a nonlinear behavior, which can be described by a quadratic function. The results of the quadratic fits are shown in Table 1. In the table, it can be seen that the high-frequency stretching modes are those with the largest pressure coefficients. In particular, the mode most sensitive to pressure is the A_g mode with frequency 918 cm^{-1} at 11.7 GPa. The fact that different modes have different pressure dependence leads to several modes gradually merging under compression. This is for instance the case of the B_g and A_g modes with frequencies 411 and 419 cm^{-1} at 11.7 GPa. They are represented by open blue symbols in Figure 3. Under compression the frequency of the B_g mode increases faster than that of the A_g mode, reducing the frequency difference between the two modes. The modes merge and cannot be distinguished above 25 GPa. Another fact to highlight is the existence of anticrossing modes. These are the B_g modes with frequencies 353 and 371 cm^{-1} at 11.7 GPa, which are shown with open red symbols to facilitate the identification of the anticrossing behavior. A final remark, is that the quadratic coefficient (ω_2)

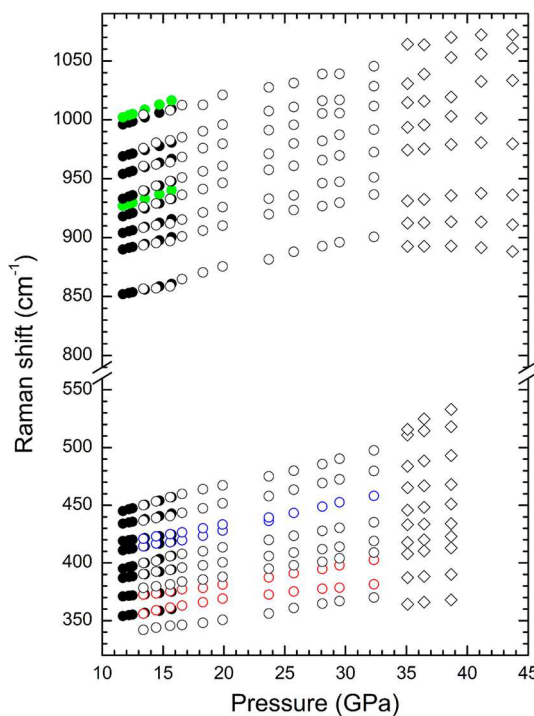


Figure 3. Pressure dependence of Raman modes in SrCrO_4 from 11 to 45 GPa. Black solid circles are from ref 10. Green solid circles are from ref 10 and correspond to overtones (see text). Open circles represent results from the present results for the AgMnO_4 -type phase. We represent in blue one A_g and one B_g mode which merges under compression. We show in red the anticrossing of two B_g . Results for the new HP phase observed beyond 35 GPa are represented with diamonds.

in the function that describes the pressure dependence of Raman modes is negative in most modes (see Table 1), with the pressure dependence having a negative curvature, decreasing the slope of the curves as pressure increases. This is particularly noticeable for the high-frequency modes; in all of them, $\omega_2 < 0$.

We now comment on the Raman spectrum of phase IV. Interestingly for this phase, we also observed 18 Raman-active modes in the frequency region covered by our measurements. The frequency of these modes and their pressure dependence are summarized in Table 2. The pressure dependence of the

Table 2. Wave Numbers (ω_0) Determined at 35.1 GPa for Raman Modes of New Phase IV of SrCrO_4 (in cm^{-1})^a

ω_0	ω_1	ω_0	ω_1
364	1.04	893	-0.46
387	0.79	913	-0.12
408	1.40	931	0.68
418	1.44	975	0.69
433	0.24	994	1.44
446	1.44	1013	2.51
465	0.76	1034	3.43
484	2.51	1064	1.10
511	1.98		
516	4.72		

^aThe pressure dependence of the frequency of each mode is described by $\omega(P) = \omega_0 + \omega_1 \Delta P$, with $\Delta P = P - 35.1$ GPa. On the left (right), the bending (stretching) modes are shown.

modes is shown in Figure 3. There, it can be seen that all modes harden under compression. Raman experiments do not allow the determination of the crystal structure of phase IV (we hope our study will trigger the X-ray diffraction experiments needed for it) but they can give some hints which can guide the search for the HP structure of phase IV. The fact that the AgMnO_4 -type structure of SrCrO_4 and phase IV have the same number of modes with a similar frequency distribution is indicative that there is little (or no) change in the coordination number of Cr and Sr at the phase transition.⁴² The fact that the high- and intermediate-frequency modes cover a wider frequency range in phase IV than in the AgMnO_4 -type phase suggest a distortion of the CrO_4 octahedron. The shift of the highest-frequency mode toward high frequency after the phase transition is suggesting a shortening of the Cr–O bond after the phase transition. This is expected to enhance the bond strength, causing an increase of the Raman stretching frequency.⁴³ The fact that there are no coordination number changes at the AgMnO_4 -type to phase IV transition suggest that the crystal structure of phase IV should be related to that of the AgMnO_4 -type phase, the transition probably being displacive, which is consistent with the fact that it is reversible.⁴⁴ A literature search indicates that there are two structures with similarities to the AgMnO_4 structure in compounds related to SrCrO_4 .^{45,46} These are the Barite (space group $Pnma$) and another orthorhombic structure described by space group $P2_12_12_1$. The first structure has the same number of Raman modes as the AgMnO_4 -type structure (11 Ag + 7 B1g + 11 B2g + 7 B3g); however, the second has 69 Raman active modes (18 A + 17 B1 + 17 B2 + 17 B3), which exclude it as a potential HP phase for SrCrO_4 . Therefore, among the two candidate structures, only Barite (a high-symmetry version of AgMnO_4) has a Raman spectrum consistent with our finding for phase IV of SrCrO_4 . A definitive identification of the crystal structure of it should be obtained in future HP X-ray diffraction experiments.

Before discussing the optical and resistivity measurements, we comment on the pressure dependence of Raman modes in phase IV. The results obtained are summarized in Figure 3. In the intermediate-frequency region, the modes can be followed up to 39 GPa before they vanished. In the high-frequency region (the most intense modes), the modes can be followed up to 45 GPa. In both regions, the pressure dependence of the frequencies is nearly linear. The frequencies at 35.1 GPa and the linear pressure coefficients (ω_1) are shown in Table 2. Notice that most modes have a smaller pressure coefficient than in the AgMnO_4 -type phase. The mode with the largest pressure coefficient is the mode with frequency 516 cm^{-1} . Interestingly, in phase IV, not all the modes harden under compression. There are two modes with negative pressure coefficients (see Table 2). The presence of such modes is usually a hint of structural instabilities,⁴⁷ which is consistent with the evidence of a pressure-induced phase transition we found at 45 GPa.

b. Optical Absorption. We now discuss the results from optical-absorption experiments. Figure 4 shows a selection of spectra measured at different pressures. The reported measurements extended the pressure range covered by previous studies¹⁰ from 14.5 to 30.7 GPa. In the previous studies, it was determined that SrCrO_4 is an indirect band gap material. Our results fully agree with those previously reported¹⁰ up to 14.5 GPa, following the absorption spectra, the quadratic dependence in energy expected for an indirect gap. From 14.5

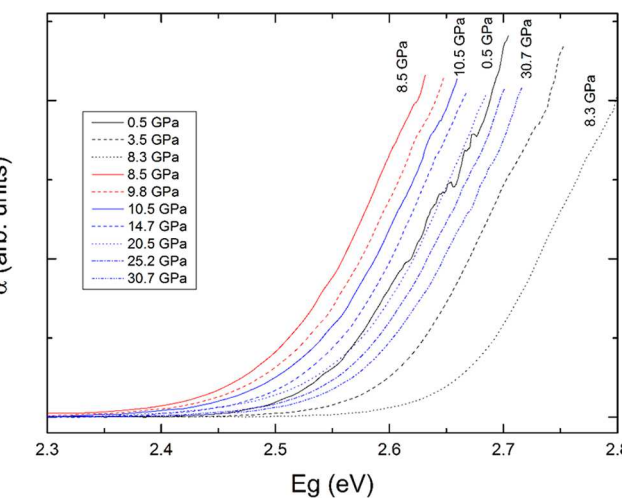


Figure 4. Optical-absorption spectra measured at different pressures. Results for different phases are shown in different colors. Experiments at different pressures are shown using different styles of lines. Pressures are indicated in the onset.

to 30.7 GPa, there are no noticeable changes in the shape of the absorption spectrum (see Figure 4); consequently, it can be assumed that SrCrO_4 is an indirect band gap material up to 30.7 GPa.

We discuss now the pressure dependence of the band gap energy (E_g) in detail. We found that the absorption edge gradually blue-shifts from ambient pressure, where the E_g is 2.45 eV to 8.3 GPa where $E_g = 2.6$ eV. At 8.5 eV, an abrupt decrease of the band gap takes place, red-shifting the absorption spectrum by 0.2 eV. The absorption spectrum of SrCrO_4 gradually shifts to higher energies upon further compression. From the absorption spectra, we determined the value of E_g at different pressures with an error of ± 0.02 eV. The results are summarized in Figure 5 and compared with previously published results.¹⁰ The agreement is quite good in the pressure range where comparison is possible. In the figure, black, red, and blue symbols are used to represent results from the three known phases of SrCrO_4 ; i.e., monazite, scheelite,

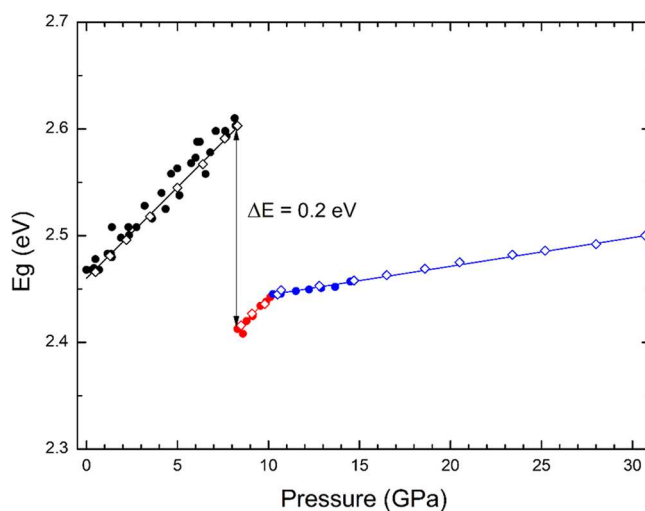


Figure 5. Pressure dependence of the band gap energy (E_g). Solid symbols are from previous experiments. Empty symbols are from present experiments. Different colors are used for different phases.

and AgMnO_4 -type. The first transition occurs at 8.5 GPa as the band gap collapses. There is a change in the evolution of band gap energy at 10.5 GPa, in agreement with the occurrence of the second transition which was detected by Raman and XRD measurements. Beyond this pressure, E_g evolves linearly with pressure up to 30.7 GPa with no evidence of phase transitions. Interestingly in the AgMnO_4 -type phase near 15 GPa E_g reaches the same value that the monazite-phase exhibits at ambient pressure. At 30.7 GPa, the value of E_g is 2.5 eV. Upon further compression, at 32.3 GPa, the crystal breaks into multiple domains which prevent the performance of absorption measurements because light becomes diffused instead of being transmitted through the sample. We suspect that the breaking of the crystal into domains is a consequence of precursor effects of the phase transition to phase IV detected by Raman experiments at 35 GPa.

We discuss now the pressure evolution of E_g . From Figures 4 and 5 it is evident that SrCrO_4 is a semiconductor material within the pressure range covered by experiments. In contrast with PbCrO_4 , the band gap of SrCrO_4 opens under compression in the monazite phase.³⁰ In accordance with band structure calculations,¹⁴ the opening of E_g in SrCrO_4 is caused by the repulsion between the Cr and O states that contribute to the top of the valence band and the bottom of the conduction band. For the case of PbCrO_4 , the contribution of Pb states to the valence and conduction bands is what favors the closing of E_g under compression.³⁰ The 0.2 eV collapse of E_g observed at the first transition (8.5 GPa) is a consequence of the change of Cr–O bond angles and distances at the monazite–scheelite transition.^{10,48} Notice that the transition modifies the global symmetry of the crystal and the Cr–O bond distances.¹⁰ These changes are reflected in the electronic structure of SrCrO_4 , which trigger the small closure of E_g found in the experiments. On the other hand, the change of the slope observed in the pressure dependence of E_g at the scheelite– AgMnO_4 -type transition (10.5 GPa) is a consequence of the change in the compressibility associated with the transition.^{10,49} Finally, the opening of E_g that takes place under compression in the two HP phases is a consequence of the volume reduction of the CrO_4 tetrahedron (as in the monazite phase) which increases the crystal field splitting between bonding and antibonding states, causing the opening of the band gap.^{50,51}

c. Resistivity. Figure 6 presents the results of the high-pressure electrical resistivity measurements. They were plotted on a semilog plot. There is a clear trend of decreasing resistivity under compression, with an overall change of more than one order of magnitude over the measured pressure range. The resistance of the sample was too high to reliably measure for pressures below 16 GPa. This is similar to the findings for PbCrO_4 .³⁰ After the phase transition to the AgMnO_4 -type phase, the resistivity becomes detectable. A change in the slope of the resistivity curve occurs near 35 GPa, which is followed by a plateau up to 42 GPa. The slope change at 35 GPa is likely connected with the previously discussed structural transition to phase IV. A second change in the slope of resistivity is present at 42 GPa, which is agreement with the transition to phase V that causes the blackening of the crystal. The data ($\rho > 80 \Omega\text{-cm}$) suggest that SrCrO_4 remains nonmetallic to at least 50 GPa.

The large resistivity observed below 16 GPa is consistent with an intrinsic semiconducting behavior of SrCrO_4 . At 300 K, assuming the same electron and hole mobility as in Si, a

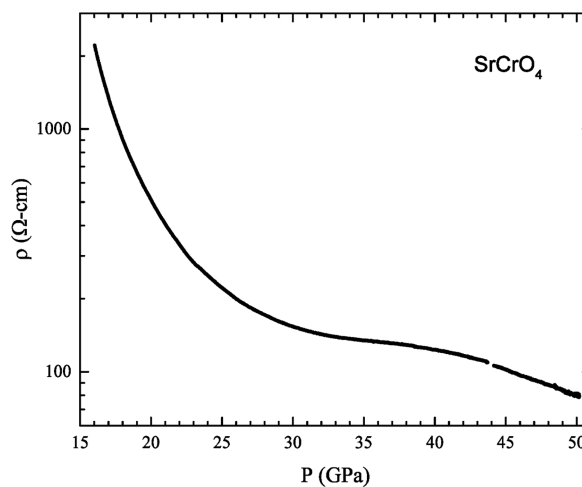


Figure 6. Resistivity versus pressure on a semilog plot. There are two changes in the slope, one near 35 GPa and the second at 42 GPa.

resistivity larger than $10^7 \Omega\text{-cm}$ is obtained for monazite-type SrCrO_4 , which explains why the resistivity was too high to be accurately measured below 16 GPa. Beyond this pressure, the most likely reason for explaining the decrease of the resistivity to detectable levels is the creation of oxygen vacancies which could act as donor levels, transferring electrons to the conduction band.^{52–54} The presence of such vacancies is typical of chromate compounds. Theoretical calculations on the related compound BiVO_4 have shown that the formation energy of oxygen vacancies can be provided by a hydrostatic pressure of 7 GPa.⁵⁵ Therefore, it is not impossible to create oxygen vacancies in SrCrO_4 at 16 GPa. These vacancies will act as donor impurities and provide n-type doping to SrCrO_4 , transforming it into an extrinsic semiconductor. As a consequence, the carrier concentration will be increased, leading to the increased conductivity, as found in oxygen-deficient NdCrO_4 , LaCrO_4 , and other compounds related to SrCrO_4 .^{52–54}

Regarding the decrease of resistivity from 16 to 35 GPa (AgMnO₄-type phase), it cannot correspond to the changes in the band gap. In fact, E_g increases under compression, as discussed in the previous section, which as a first approximation should produce an increase of resistivity. There are several reasons that could explain the decrease of resistivity. One is the enhancement of contacts between grains and the triggering of percolation effects due to compression, two facts that were recently shown to favor the decrease of resistivity in compressed powder samples like the one here used.⁵⁶ A second possible reason is that under compression, the donors that contribute free electrons to the conduction band transform from deep to shallow, leading to an increase of the carrier concentration and the consequent decrease of resistivity.^{57,58} Regarding the plateau observed in the resistivity from 35 to 42 GPa and the slope change found at 42 GPa, we can only state that they indicate a change in the electrical properties of SrCrO_4 , which is consistent with the two new phase transitions found in Raman experiments. The value of the resistivity found at the highest pressure 80 $\Omega\text{-cm}$ (at 50 GPa) is an order of magnitude larger than the expected resistivity of a metal. Therefore, this excludes the possibility that the sample blackening described before could be caused by metallization. Taking this into account, a possible explanation for SrCrO_4 becoming black would be the

formation of extrinsic defects, a phenomenon observed under high pressure in InSe and GaSe^{24,59} at pressures much lower than the metallization pressure.

4. CONCLUDING REMARKS

In this work, we reported a high pressure experimental study of SrCrO_4 . Raman, optical absorption, and resistivity measurements were carried out, expanding on the previous work performed¹⁰ by exploring a much higher pressure range. Two further transitions at 35 and 48 GPa were detected in addition to the previously observed transitions at 9 and 14 GPa. The phase V formed at 48 GPa is not fully characterized; we believe that it is not an amorphous phase, on account of the reversibility of the transition, but that a high level of structural disorder may be present. The pressure dependence of Raman active modes was discussed for two of the HP phases. In addition, optical-absorption experiments allowed the characterization of the band gap of SrCrO_4 up to 30.7 GPa (doubling the pressure range covered previously¹⁰), showing that SrCrO_4 is a semiconductor. Important contributions in this work are the resistivity measurements and the confirmation that SrCrO_4 remains a nonmetallic material at 50 GPa. The results shown further enhance our understanding of the high-pressure behavior of monazite-type oxides and ternary compounds and can have implications in geochronology and petrology as monazite-type oxides are key accessory minerals for metamorphic rocks.⁶⁰

■ AUTHOR INFORMATION

Corresponding Author

*E-mail: J.E.Proctor@salford.ac.uk.

ORCID

Daniel Errandonea: [0000-0003-0189-4221](https://orcid.org/0000-0003-0189-4221)

John E. Proctor: [0000-0003-3639-8295](https://orcid.org/0000-0003-3639-8295)

Marco Bettinelli: [0000-0002-1271-4241](https://orcid.org/0000-0002-1271-4241)

Notes

The authors declare no competing financial interest.

■ ACKNOWLEDGMENTS

The authors thank the financial support of this research from the Spanish Ministerio de Economía y Competitividad (MINECO), the Spanish Research Agency (AEI), and the European Fund for Regional Development (FEDER) under Grants MAT2016-75586-C4-1-P and MAT2015-71070-REDC (MALTA Consolider). High-pressure electrical resistivity measurements were supported by NSF CAREER DMR-1453752. M.A.H. would like to acknowledge the award of a University of Salford Doctoral Scholarship.

■ REFERENCES

- Yin, J.; Zou, Z.; Ye, J. Photophysical and photocatalytic properties of new photocatalysts MCrO_4 ($\text{M} = \text{Sr, Ba}$). *Chem. Phys. Lett.* **2003**, *378*, 24–28.
- Belyi, M. U.; Nedel'ko, S. G.; Chukova, O. V. Luminescent properties of chromates of alkali metals. *J. Appl. Spectrosc.* **1995**, *62*, 604–611.
- Chen, P.; Wu, Q. S.; Ding, Y. P.; Yuan, P. S. Synthesis of SrCrO_4 nanostructures by onion inner-coat template and their optical properties. *Bull. Mater. Sci.* **2008**, *31*, 603–608.
- Bharat, L. K.; Reddy, L. S.; Yu, J. S. Sol–gel synthesis, characterization and photocatalytic properties of SrCrO_4 particles. *Mater. Lett.* **2015**, *144*, 85–89.
- Effenberger, H.; Pertlik, F. Four monazite type structures: comparison of SrCrO_4 , SrSeO_4 , PbCrO_4 (crocoite), and PbSeO_4 . *Zeitschrift für Kristallographie* **1986**, *176*, 75–83.
- Tablero, C. Optoelectronic property analysis of MCrO_4 ($\text{M} = \text{Ba, Sr}$) with a response to visible light irradiation. *Theor. Chem. Acc.* **2015**, *134*, 72.
- Errandonea, D.; Muñoz, A.; Rodriguez-Hernandez, P.; Proctor, J.; Sapiña, F.; Bettinelli, M. Theoretical and Experimental Study of the Crystal Structures, Lattice Vibrations, and Band Structures of Monazite-Type PbCrO_4 , PbSeO_4 , SrCrO_4 , and SrSeO_4 . *Inorg. Chem.* **2015**, *54*, 7524–7535.
- Parhi, P.; Manivannan, V. Novel microwave initiated synthesis of Zn_2SiO_4 and MCrO_4 ($\text{M} = \text{Ca, Sr, Ba, Pb}$). *J. Alloys Compd.* **2009**, *469*, 558–564.
- Otero, V.; Campos, M. F.; Pinto, J. V.; Vilarigues, M.; Carlyle, L.; Melo, M. J. Barium, zinc and strontium yellows in late 19th–early 20th century oil paintings. *Heritage Sci.* **2017**, *5*, 46.
- Gleissner, J.; Errandonea, D.; Segura, A.; Pellicer-Porres, J.; Hakeem, M. A.; Proctor, J. E.; Raju, S. V.; Kumar, R. S.; Rodriguez-Hernandez, P.; Muñoz, A.; Lopez-Moreno, S.; Bettinelli, M. Monazite-type SrCrO_4 under compression. *Phys. Rev. B: Condens. Matter Mater. Phys.* **2016**, *94*, 134108.
- Errandonea, D.; Popescu, C.; Garg, A. B.; Botella, P.; Martinez-Garcia, D.; Pellicer-Porres, J.; Rodriguez-Hernandez, P.; Muñoz, A.; Cuenca-Gotor, V.; Sans, J. A. Pressure-induced phase transition and band-gap collapse in the wide-band-gap semiconductor InTaO_4 . *Phys. Rev. B: Condens. Matter Mater. Phys.* **2016**, *93*, 035204.
- Ruiz-Fuertes, J.; Lopez-Moreno, S.; Lopez-Solano, J.; Errandonea, D.; Segura, A.; Laomba-Perales, R.; Muñoz, A.; Radescu, S.; Rodriguez-Hernandez, P.; Gospodinov, M.; Nagornaya, L. L.; Tu, C. Y. Pressure effects on the electronic and optical properties of AWO_4 wolframites ($\text{A} = \text{Cd, Mg, Mn, and Zn}$): The distinctive behavior of multiferroic MnWO_4 . *Phys. Rev. B: Condens. Matter Mater. Phys.* **2012**, *86*, 125202.
- Ruiz-Fuertes, J.; Friedrich, A.; Errandonea, D.; Segura, A.; Morgenroth, W.; Rodriguez-Hernandez, P.; Muñoz, A.; Meng, Y. Optical and structural study of the pressure-induced phase transition of CdWO_4 . *Phys. Rev. B: Condens. Matter Mater. Phys.* **2017**, *95*, 174105.
- Errandonea, D. High-pressure phase transitions and properties of MTO_4 compounds with the monazite-type structure. *Phys. Status Solidi B* **2017**, *254*, 1700016.
- Garg, A. B.; Errandonea, D.; Popescu, C.; Martinez-Garcia, D.; Pellicer-Porres, J.; Rodriguez-Hernandez, P.; Muñoz, A.; Botella, P.; Cuenca-Gotor, V. P.; Sans, J. A. Pressure-Driven Isostructural Phase Transition in InNbO_4 : In Situ Experimental and Theoretical Investigations. *Inorg. Chem.* **2017**, *56*, 5420–5430.
- Redfern, S. A. T. Length scale dependence of high-pressure amorphization: the static amorphization of anorthite. *Mineral. Mag.* **1996**, *60*, 493–498.
- Garg, A. B.; Shanavas, K. V.; Surinder, B. N. W.; Sharma, M. Phase transition and possible metallization in CeVO_4 under pressure. *J. Solid State Chem.* **2013**, *203*, 273–280.
- Grzechnik, A.; Crichton, W. A.; Hanfland, M. SrWO_4 at high pressures. *Phys. Status Solidi B* **2005**, *242*, 2795–2802.
- Dewaele, A.; Torrent, M.; Loubeire, P.; Mezouar, M. Compression curves of transition metals in the Mbar range: Experiments and projector augmented-wave calculations. *Phys. Rev. B: Condens. Matter Mater. Phys.* **2008**, *78*, 104102.
- Tateiwa, N.; Haga, Y. Evaluations of pressure-transmitting media for cryogenic experiments with diamond anvil cell. *Rev. Sci. Instrum.* **2009**, *80*, 123901.
- Errandonea, D.; Muñoz, A.; Gonzalez-Platas, J. High-pressure x-ray diffraction study of $\text{YBO}_3/\text{Eu}^{3+}$, GdBO_3 , and EuBO_3 : Pressure-induced amorphization in GdBO_3 . *J. Appl. Phys.* **2014**, *115*, 216101.
- Errandonea, D. Exploring the properties of MTO_4 compounds using high-pressure powder x-ray diffraction. *Cryst. Res. Technol.* **2015**, *50*, 729.

(23) Proctor, J. E.; Maynard-Casely, H. E.; Hakeem, M. A.; Cantiah, D. Raman spectroscopy of methane (CH_4) to 165 GPa: Effect of structural changes on Raman spectra. *J. Raman Spectrosc.* **2017**, *48*, 1777–1782.

(24) Errandonea, D.; Boehler, R.; Japel, S.; Mezouar, M.; Benedetti, L. R. Structural transformation of compressed solid Ar: An x-ray diffraction study to 114 GPa. *Phys. Rev. B: Condens. Matter Mater. Phys.* **2006**, *73*, 092106.

(25) Panchal, V.; Garg, N.; Poswal, H. K.; Errandonea, D.; Rodriguez-Hernandez, P.; Muñoz, A.; Cavalli, E. High-pressure behavior of CaMoO_4 . *Physical Review Materials* **2017**, *1*, 043605.

(26) Segura, A.; Sans, J. A.; Errandonea, D.; Martinez-Garcia, D.; Fages, V. High conductivity of Ga-doped rock-salt ZnO under pressure: Hint on deep-ultraviolet-transparent conducting oxides. *Appl. Phys. Lett.* **2006**, *88*, 011910.

(27) Panchal, V.; Errandonea, D.; Segura, A.; Rodriguez-Hernandez, P.; Muñoz, A.; Lopez-Moreno, S.; Bettinelli, M. The electronic structure of zircon-type orthovanadates: Effects of high-pressure and cation substitution. *J. Appl. Phys.* **2011**, *110*, 043723.

(28) Errandonea, D.; Martinez-Garcia, D.; LaComba-Perales, R.; Ruiz-Fuertes, J.; Segura, A. Effects of high pressure on the optical absorption spectrum of scintillating PbWO_4 crystals. *Appl. Phys. Lett.* **2006**, *89*, 091913.

(29) Weir, S. T.; Jackson, D. D.; Falabella, S.; Samudrala, G.; Vohra, Y. K. An electrical microheater technique for high-pressure and high-temperature diamond anvil cell experiments. *Rev. Sci. Instrum.* **2009**, *80*, 013905.

(30) Errandonea, D.; Bandiello, E.; Segura, A.; Hamlin, J. J.; Maple, M. B.; Rodriguez-Hernandez, P.; Muñoz, A. Tuning the band gap of PbCrO_4 through high-pressure: Evidence of wide-to-narrow semiconductor transitions. *J. Alloys Compd.* **2014**, *587*, 14–20.

(31) Zocco, D. A.; Hamlin, J. J.; Sayles, T. A.; Maple, M. B.; Chu, J.-H.; Fisher, I. R. High-pressure, transport, and thermodynamic properties of CeTe_3 . *Phys. Rev. B: Condens. Matter Mater. Phys.* **2009**, *79*, 134428.

(32) Garg, A. B.; Errandonea, D.; Rodríguez-Hernández, P.; Muñoz, A. ScVO_4 under non-hydrostatic compression: a new metastable polymorph. *J. Phys.: Condens. Matter* **2017**, *29*, 055401.

(33) Bandiello, E.; Errandonea, D.; Martinez-Garcia, D.; Santamaría-Perez, D.; Manjón, F. J. Effects of high-pressure on the structural, vibrational, and electronic properties of monazite-type PbCrO_4 . *Phys. Rev. B: Condens. Matter Mater. Phys.* **2012**, *85*, 024108.

(34) Manjón, F. J.; Errandonea, D.; Segura, A.; Chervin, J. C.; Muñoz, V. Precursor effects of the Rhombohedral-to-Cubic Phase Transition in Indium Selenide. *High Pressure Res.* **2002**, *22*, 261.

(35) Higuchi, M.; Chuman, Y.; Kodaira, K. Relation between phase transitions and crack formation in lithium orthovanadate single crystals. *J. Mater. Sci. Lett.* **2001**, *20*, 1655–1656.

(36) Kolobov, A. V.; Krbal, M.; Fons, P.; Tominaga, J.; Uruga, T. Distortion-triggered loss of long-range order in solids with bonding energy hierarchy. *Nat. Chem.* **2011**, *3*, 311–316.

(37) Arora, A. K. Pressure-induced amorphization versus decomposition. *Solid State Commun.* **2000**, *115*, 665–668.

(38) Twu, J.; Shih, C. F.; Guo, T. H.; Chen, K. H. Raman spectroscopic studies of the thermal decomposition mechanism of ammonium metavanadate. *J. Mater. Chem.* **1997**, *7*, 2273–2277.

(39) Lin, T.; Li, Y.; Xu, Y.; Lan, G.; Wang, H. Raman-scattering study on pressure amorphization of LiNbO_3 crystal. *J. Appl. Phys.* **1995**, *77*, 3584.

(40) Hanfland, M.; Proctor, J. E.; Guillaume, C. L.; Degtyareva, O.; Gregoryanz, E. High-Pressure Synthesis, Amorphization, and Decomposition of Silane. *Phys. Rev. Lett.* **2011**, *106*, 095503.

(41) Grzegorczyk, A.; Wolf, G. H.; McMillan, P. F. J. Raman scattering study of SrTiO_3 at high pressure. *J. Raman Spectrosc.* **1997**, *28*, 885–889.

(42) Ruschel, K.; Nasdala, L.; Kronz, A.; Hanchar, J. M.; Többens, M.; Skoda, R.; Finger, F.; Möller, A. A Raman spectroscopic study on the structural disorder of monazite-(Ce). *Mineral. Petrol.* **2012**, *105*, 41–55.

(43) Weckhuysen, B. M.; Wachs, I. E. Raman spectroscopy of supported chromium oxide catalysts. Determination of chromium–oxygen bond distances and bond orders. *J. Chem. Soc., Faraday Trans.* **1996**, *92*, 1969–1973.

(44) Daniel, I.; Gillet, P.; Ghose, S. A new high-pressure phase transition in anorthite ($\text{CaAl}_2\text{Si}_2\text{O}_8$) revealed by Raman spectroscopy. *Am. Mineral.* **1995**, *80*, 645–648.

(45) Ruiz-Fuertes, J.; Hirsch, A.; Friedrich, A.; Winkler, B.; Bayarjargal, L.; Morgenroth, W.; Peters, L.; Roth, G.; Milman, V. High-pressure phase of LaPO_4 studied by x-ray diffraction and second harmonic generation. *Phys. Rev. B: Condens. Matter Mater. Phys.* **2016**, *94*, 134109.

(46) Errandonea, D.; Kumar, R. S.; Achary, S. N.; Tyagi, A. K. In situ high-pressure synchrotron x-ray diffraction study of CeVO_4 and TbVO_4 up to 50 GPa. *Phys. Rev. B: Condens. Matter Mater. Phys.* **2011**, *84*, 224121.

(47) Errandonea, D.; Pellicer-Porres, J.; Pujol, M. C.; Carvajal, J. J.; Aguiló, M. Room-temperature vibrational properties of potassium gadolinium double tungstate under compression up to 32 GPa. *J. Alloys Compd.* **2015**, *638*, 14–20.

(48) Benmakhlof, A.; Errandonea, D.; Bouchenafa, M.; Maabed, S.; Bouhemadou, A.; Bentabet, A. New pressure-induced polymorphic transitions of anhydrous magnesium sulfate. *Dalton Trans.* **2017**, *46*, 5058–5068.

(49) Chang, K. J.; Froyen, S.; Cohen, M. L. Pressure coefficients of band gaps in semiconductors. *Solid State Commun.* **1984**, *50*, 105–107.

(50) Errandonea, D.; Martinez-Garcia, D.; LaComba-Perales, R.; Ruiz-Fuertes, J.; Segura, A. Effects of high pressure on the optical absorption spectrum of scintillating PbWO_4 crystals. *Appl. Phys. Lett.* **2006**, *89*, 091913.

(51) Stoltzfus, M. W.; Woodward, P. M.; Seshadri, R.; Klepeis, J. H.; Bursten, B. Structure and Bonding in SnWO_4 , PbWO_4 , and BiVO_4 : Lone Pairs vs Inert Pairs. *Inorg. Chem.* **2007**, *46*, 3839–3850.

(52) Aoki, Y.; Konno, H.; Tachikawa, H. The electronic and magnetic properties of LaCrO_4 and $\text{Nd}_{1-x}\text{Ca}_x\text{CrO}_4$ ($x = 0$ –0.2) and the conduction mechanism. *J. Mater. Chem.* **2001**, *11*, 1214–1221.

(53) BJORHEIM, T. S.; NORBY, T. Haugsrud, Hydration and proton conductivity in LaAsO_4 . *R. J. Mater. Chem.* **2012**, *22*, 1652.

(54) Williams, M. L.; Jercinovic, M. J.; Hetherington, C. J. Microprobe monazite geochronology: understanding geologic processes by integrating composition and chronology. *Annu. Rev. Earth Planet. Sci.* **2007**, *35*, 137–175.

(55) Huang, Y.; Yuan, Y.; Ma, F.; Zhang, Z.; Wei, X.; Zhu, G. Structural stability, electronic, and optical properties of BiVO_4 with oxygen vacancy under pressure. *Phys. Status Solidi B* **2017**, *1700653*.

(56) Creyssels, M.; Laroche, C.; Falcon, E.; Castaing, B. Pressure dependence of the electrical transport in granular materials. *Eur. Phys. J. E: Soft Matter Biol. Phys.* **2017**, *40*, 56.

(57) Errandonea, D.; Segura, A.; Sanchez-Royo, J. F.; Muñoz, V.; Grima, P.; Chevy, A.; Ulrich, C. Investigation of conduction-band structure, electron-scattering mechanisms, and phase transitions in indium selenide by means of transport measurements under pressure. *Phys. Rev. B: Condens. Matter Mater. Phys.* **1997**, *55*, 16217.

(58) Errandonea, D.; Segura, A.; Manjón, F. J.; Chevy, A. Transport measurements in InSe under high pressure and high temperature: shallow-to-deep donor transformation of Sn related donor impurities. *Semicond. Sci. Technol.* **2003**, *18*, 241.

(59) Rizzo, A.; De Blasi, C.; Catalano, M.; Cavalieri, P. Dislocations in $\text{Al}_{11}\text{B}_6\text{VI}$ single crystals. *Phys. Stat. Sol. A* **1988**, *105*, 101–112.

(60) Wang, J. M.; Wu, F. Y.; Rubatto, D.; Liu, S. R.; Zhang, J. J.; Liu, X. C.; Yang, L. Monazite behaviour during isothermal decompression in pelitic granulites: a case study from Dingye, Tibetan Himalaya. *Contrib. Mineral. Petrol.* **2017**, *172*, 81.